The Role of Bulky Substituents in Brookhart-Type Ni(II) Diimine Catalyzed Olefin Polymerization: A Combined Density Functional Theory and Molecular Mechanics Study

Liqun Deng,[†] Tom K. Woo,[†] Luigi Cavallo,[‡] Peter M. Margl,[†] and Tom Ziegler*[,†]

Contribution from the Department of Chemistry, University of Calgary, 2500 University Drive, N.W., T2N 1N4, Calgary, Alberta, Canada, and Dipartimento di Chimica, Università "Federico II" di Napoli, Via Mezzocannone 4, I-80134, Napoli, Italy

Received January 24, 1997. Revised Manuscript Received April 7, 1997[⊗]

Abstract: The role of the bulky ligands in Ni(II) diimine catalyzed ethylene polymerization has been examined with a combined density functional theory quantum mechanics and molecular mechanics (QM/MM) model. Specifically, we have examined the catalytic center of the type $(ArN{=}C(R){-}C(R){=}NAr)Ni^{II}\text{-}R'^{+}$, where R = Me and Ar = 2,6-$C_6H_3(i\text{-}Pr)_2$. The Ar and R groups were treated by a molecular mechanics force field while density functional theory was applied to the remainder of the system. The chain propagation, chain branching, and chain termination processes have been investigated with the hybrid method and found to have barriers of $\Delta H^{\ddagger} = 11.8$, 15.3, and 18.4 kcal/mol, respectively, which is in excellent agreement with experiment in both absolute and relative terms. This is in stark contrast to the pure QM model in which the influence of the bulky Ar and R groups was neglected and the established order of the barriers is not even reproduced. The role played by the bulky substituents is dual in nature. First, the Ar and R groups act to sterically hinder the axial coordination sites of the Ni center. This has the most dramatic destabilizing effect on the resting state and termination transition states, in which both axial positions are occupied. In addition to the steric factor, we find that the electronic preference for the aryl rings to orient themselves in a coplanar fashion with the diimine ring results in a stabilization of the insertion transition state relative to the resting state. These two factors act to both lower the propagation barrier and increase the termination barrier compared to the "naked" pure QM model system.

1. Introduction

Brookhart and co-workers[1−3] have recently developed Ni(II) and Pd(II) diimine based catalysts of the type $(ArN{=}C(R){-}C(R){=}NAr)M{-}CH_3^{+}$, which have emerged as promising alternatives to both Ziegler−Natta systems and metallocene catalysts for olefin polymerization. Traditionally, such late metal catalysts are found to produce dimers or extremely low molecular weight oligomers due to the favorability of the β-elimination chain termination process.[4] With the Brookhart systems very high molecular weight polymers can be produced. They also exhibit high activities which are competitive with commercial metallocene catalysts.[5] Not only can these catalysts convert ethylene into high molecular weight polyethylene, but the polymers also exhibit a controlled level of short-chain branching. NMR studies which indicate the presence of multiple methine, methylene, and methyl signals suggests branches of variable length with methyl branches predominating.[1] The extent of the branching is a function of temperature, monomer concentration, and catalyst structure. Thus, by simply varying these parameters, polymers which are highly branched or virtually linear can be tailored.

Brookhart's group has studied the mechanistic details of the polymerization including the role of the bulky substituents on the diimine ligands.[1,2] Three main processes are thought to dominate the polymerization chemistry of these catalyst systems, namely propagation, chain branching, and chain termination. Following cocatalyst activation of the precatalyst, a diimine methyl cation is formed. First insertion of ethylene yields a diimine alkyl cation, which upon uptake of another ethylene molecule produces a metal alkyl olefin π-complex. This π-complex has been established by NMR studies[1] to be the catalytic resting state of the system. The chain propagation cycle is depicted in Scheme 1. The first step involves the insertion of the coordinated olefin moiety to form a metal alkyl cationic species. Rapid uptake of monomer returns the system to the initial resting state π-complex. The unique short-chain branching observed with these catalysts is proposed to occur via an alkyl chain isomerization process as sketched in Scheme 2. In this proposed process, β-hydride elimination first yields a putative hydride olefin π-complex. Rotation of the π-coor-

Scheme 1

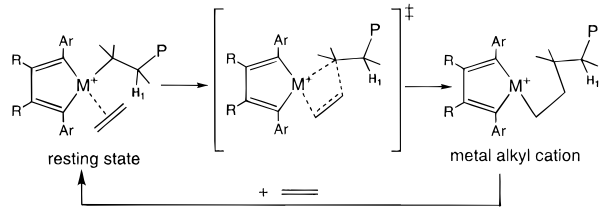

Scheme 2

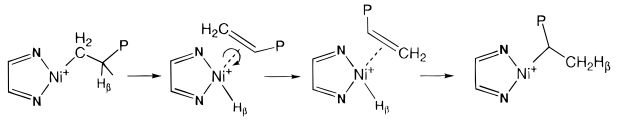

[†] University of Calgary.
[‡] Università "Federico II" di Napoli.
[⊗] Abstract published in *Advance ACS Abstracts,* June 15, 1997.

(1) Johnson, L. K.; Killian, C. M.; Brookhart, M. *J. Am. Chem. Soc.* **1995**, *117*, 6414.
(2) Johnson, L. K.; Mecking, S.; Brookhart, M. *J. Am. Chem. Soc.* **1996**, *118*, 267.
(3) Killian, C. M.; Tempel, D. J.; Johnson, L. K.; Brookhart, M. *J. Am. Chem. Soc.* **1996**, *118*, 11664.
(4) Wilke, G. *Angew. Chem., Int. Ed. Engl.* **1988**, *27*, 185.
(5) Haggin, J. *Chem. Eng. News* **1996**, *Feb 5*, 6.

S0002-7863(97)00226-6 CCC: $14.00

Scheme 3

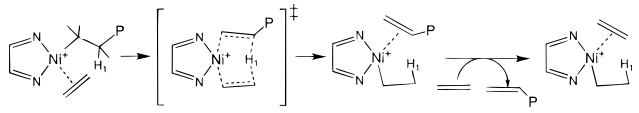

dinated olefin moiety about its coordination axis followed by reinsertion produces a secondary carbon unit and therefore a branching point. Consecutive repetition of this process allows the metal center to migrate down the polymer chain, thus producing longer chain branches. Chain termination occurs via monomer assisted β-hydrogen elimination, either in a fully concerted fashion as illustrated in Scheme 3 or in a multistep associative mechanism as implicated by Johnson *et al.*[1]

Similar Ni and Pd catalysts developed by Keim[6] and others[7,8] which do not posses the bulky ligand systems have been used to produce dimers or extremely low molecular weight oligomers.[9] Brookhart has suggested[1] that the bulky aryl ligands act to preferentially block the axial sites of the metal center as illustrated by Figure 1. This feature in the catalyst system must in some way act to retard the chain termination process relative to the propagation process, thereby allowing these catalysts to produce high molecular weight polymers.

In an earlier pure quantum mechanical study[10,11] we neglected the role of the bulky diimine substituents by modeling the catalyst system with a Ni(II) coordinated to an unsubstituted diimine ligand (HN═CH−CH═NH). With this unsubstituted model system, the chain termination process was found to be more favorable than the propagation and therefore the catalyst would not produce the high molecular weight polymers as demonstrated by Brookhart's catalyst. Rather, the model system would only be useful as a dimerization catalyst. The barriers for propagation, chain isomerization (branching), and chain termination were calculated to be $\Delta H^{\ddagger} = 16.8$, 12.8, and 9.7 kcal/mol, respectively. Although the truncated model system did not reproduce the established order of the barrier heights, the structure of the optimized transition states did offer insights into the role of the bulky ligands. As suspected by Johnson *et al.*, the transition state for chain termination occupies both axial positions of the metal whereas the insertion transition states only occupy the equatorial coordination sites. Thus, the bulky aryl substituents likely destabilize the transition state of the termination process more so than the insertion transition state.

In this study we intend to examine, in a detailed manner, the role of the bulky diimine substituents in the Brookhart catalyst system with the combined quantum mechanics/molecular mechanics (QM/MM) approach[12−14] of Morokuma and Maseras.[12] With the QM/MM method, part of the molecular system, namely the active site, is treated quantum mechanically while the remainder of the system is treated with a molecular mechanics force field. This allows extremely large systems which are out of the reach of pure QM calculations to be studied in an efficient and detailed manner. In this study, we will examine the (ArN═C(R)−C(R)═NAr)Ni^{II} based catalyst system where R = methyl and Ar = 2,6-C_6H_3(*i*-Pr)$_2$. The bulky R and Ar groups will be treated by a molecular mechanics potential while the remainder of the system will be described by a density functional potential.

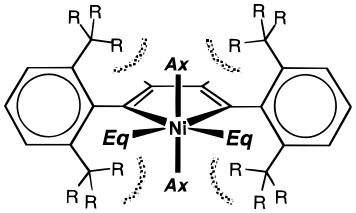

Figure 1. Axial (*Ax*) and equatorial (*Eq*) coordination sites of the metal center and their potential steric interactions with the bulky substituents.

2. Computational Details

Stationary points on the potential energy surface were calculated with the Amsterdam Density Functional (ADF) program system, developed by Baerends *et al.*[15,16] and vectorized by Ravenek.[17] The numerical integration scheme applied for the calculations was developed by te Velde *et al.*[18] The geometry optimization procedure was based on the method from Versluis and Ziegler.[19] The electronic configurations of the molecular systems were described by a triple-ζ basis set on nickel[20,21] for 3s, 3p, 3d, 4s, and 4p. Double-ζ STO basis sets were used for carbon (2s, 2p), hydrogen (1s), and nitrogen (2s, 2p), augmented with a single 3d polarization function except for hydrogen where a 2p function was used. The $1s^2 2s^2 2p^6$ configuration on nickel and the $1s^2$ shell on carbon and nitrogen were assigned to the core and treated within the frozen core approximation. A set of auxiliary[22] s, p, d, f, and g STO functions, centered on all nuclei, was used in order to fit the molecular density and present Coulomb and exchange potentials accurately in each SCF cycle. Energy differences were calculated by augmenting the local exchange-correlation potential by Vosko *et al.*[23] with Becke's[24] nonlocal exchange corrections and Perdew's[25,26] nonlocal correlation correction. Geometries were optimized including nonlocal corrections. First-order scalar relativistic corrections[27,28] were added to the total energy, since a perturbative relativistic approach is sufficient for 3d metals. In view of the fact that all systems investigated in this work show a large HOMO-LUMO gap, a spin restricted formalism was used for all calculations.

The ADF program system was modified[29] to include the AMBER95[30] molecular mechanics force field according to the method prescribed by Morokuma and Maseras.[12] Using the terminology introduced by Morokuma,[12] Chart 1 defines the four sets of QM/MM atom types in the real system and the QM model system. Set 1 represents the QM atoms that are common to both the model system and the real system.

(6) Keim, W. *Angew. Chem., Int. Ed. Engl.* **1990**, *29*, 235.
(7) Abecywickrema, R.; Bennett, M. A.; Cavell, K. J.; Kony, M.; Masters, A. F.; Webb, A. G. *J. Chem. Soc., Dalton Trans.* **1993**, 59.
(8) Brown, S. J.; Masters, A. F. *J. Organomet. Chem.* **1989**, *367*, 371.
(9) These systems have been calculated theoretically by Fan and Ziegler: (a) Fan, L.; Krzywicki, A.; Somogyvari, A.; Ziegler, T. *Inorg. Chem.* **1994**, *33*, 5287. (b) Fan, L.; Krzywicki, A.; Somogyvari, A.; Ziegler, T. *Inorg. Chem.* **1996**, *25*, 4003.
(10) Deng, L.; Margl, P. M.; Ziegler, T. *J. Am. Chem. Soc.* **1997**, *119*, 1094.
(11) Since submission of this paper, another pure QM study of the same process has been published: Musaev, D. G.; Froese, R. D. J.; Svensson, M.; Morokuma, K. *J. Am. Chem. Soc.* **1997**, *119*, 367.
(12) Maseras, F.; Morokuma, K. *J. Comput. Chem.* **1995**, *16*, 1170.
(13) Singh, U. C.; Kollman, P. A. *J. Comput. Chem.* **1986**, *7*, 718.
(14) Field, M. J.; Bash, P. A.; Karplus, M. *J. Comput. Chem.* **1990**, *11*, 700.
(15) Baerends, E. J.; Ellis, D. E.; Ros, P. *Chem. Phys.* **1973**, *2*, 41.
(16) Baerends, E. J.; Ros, P. *Chem. Phys.* **1973**, *2*, 52.
(17) Ravenek, W. *Algorithms and Applications on Vector and Parallel Computers*; te Riele, H. J. J., Dekker, T. J., van de Horst, H. A., Eds.; Elsevier: Amsterdam, The Netherlands, 1987.
(18) te Velde, G.; Baerends, E. J. *J. Comput. Chem.* **1992**, *99*, 84.
(19) Versluis, L.; Ziegler, T. *J. Chem. Phys.* **1988**, *88*, 322.
(20) Snijders, J. G.; Baerends, E. J.; Vernoijs, P. *At. Nucl. Data Tables* **1982**, *26*, 483.
(21) Vernoijs, P.; Snijders, J. G.; Baerends, E. J. *Slater Type Basis Functions for the Whole Periodic System*; Department of Theoretical Chemistry, Free University: Amsterdam, The Netherlands, 1981.
(22) Krijn, J.; Baerends, E. J. *Fit Functions in the HFS Method*; Department of Theoretical Chemistry, Free University: Amsterdam, The Netherlands, 1984.
(23) Vosko, S. H.; Wilk, L.; Nusair, M. *Can. J. Phys.* **1980**, *58*, 1200.
(24) Becke, A. *Phys. Rev. A* **1988**, *38*, 3098.
(25) Perdew, J. P.; Zunger, A. *PRB* **1981**, *23*, 5048.
(26) Perdew, J. P. *Phys. Rev. B* **1986**, *34*, 7406.
(27) Snijders, J. G.; Baerends, E. J. *Mol. Phys.* **1978**, *36*, 1789.
(28) Snijders, J. G.; Baerends, E. J.; Ros, P. *Mol. Phys.* **1979**, *38*, 1909.
(29) Woo, T. K.; Cavallo, L.; Ziegler, T. Unpublished work.
(30) Cornell, W. D.; Cieplak, P.; Bayly, C. I.; Gould, I. R.; Merz, K. M., Jr.; Ferguson, D. M.; Spellmeyer, D. C.; Fox, T.; Caldwell, J. W.; Kollman, P. A. *J. Am. Chem. Soc.* **1995**, *117*, 5179.

Chart 1

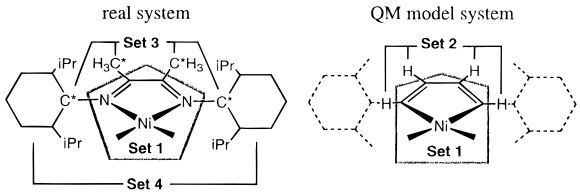

Set 1 also includes the growing alkyl chain, and the ethene monomer. The set 2 atoms or the so called capping "dummy" hydrogen atoms are only present in the model system. These dummy atoms are replaced in the real system by the corresponding set 3 atoms or "linking" carbon atoms. These set 3 carbon atoms are denoted by an asterisk in Chart 1. The set 4 atoms or the pure MM atoms encompass the remainder of the system, namely the R and Ar substituents. The rules determining which MM energy and gradient contributions to omit are defined in ref 12. For each covalent bond that crosses the QM-MM boundary, such as the N−C* bond of Chart 1, there are two bond lengths to consider which are coupled to one another. The bond between the set 1 atom and the set 4 atom and the other between the set 1 atom and the set 2 atom are coupled such that their difference, ΔR, is fixed. In the present case, the difference between the two bond lengths was fixed to $\Delta R = 0.41$ Å for the R substituents giving a C−C bond of roughly 1.51 Å and fixed to $\Delta R = 0.35$ Å for the Ar substituents providing a N−C(aryl) distance of roughly 1.38 Å.

An augmented AMBER95 force field[30] was utilized to describe the molecular mechanics potential. (All force field parameters are provided as Supporting Information.) Employing the AMBER atom type labels as described in ref 30, the diimine carbon was assigned with atom type "CM" parameters, the diimine N with "N2", aryl ring carbon atoms with "CA", aryl ring hydrogen atoms with "HA", and the remaining carbon and hydrogen atoms of the MM region with "CT" and "HC", respectively. For the propagation and termination processes, the reacting ethene monomer was assigned with sp^2 "RC" van der Waals parameters through to the transition state structure and changed to sp^3 "CT" parameters in the product. A similar procedure was followed for the isomerization process. Alkyl carbon and hydrogen atoms of the active site were assigned "CT" and "HC" van der Waals parameters, respectively. Ni was assigned the "Ni4+2" van der Waals parameters of Rappé's UFF.[31] Electrostatic interactions were not included in the molecular mechanics potential.

All structures shown correspond to minimum points on the potential surface, except those prefixed by **TS**, which represent transition states. Transition states were obtained by full transition state optimization. No symmetry constraints were used. All reported linear transit calculations involve full geometry optimization along a reaction coordinate that is constrained in each step. We have recently verified the accuracy of our DFT approach in a very similar Pd(II) system, where the barrier heights were found to be within 3−5 kcal/mol of experimental measurements.[32,33] Stanton and Merz have undertaken a systematic study of the reliability of DFT calculations for barrier heights and have concluded that DFT yields results of the same quality as post-HF calculations.[34] In a number of previous papers, transition metal−ligand dissociation energetics have been proven to be correct within 5 kcal/mol of the experimental result.[35−39] The combined or integrated QM/MM method has recently been applied to organometallic systems by Morokuma and co-workers.[40]

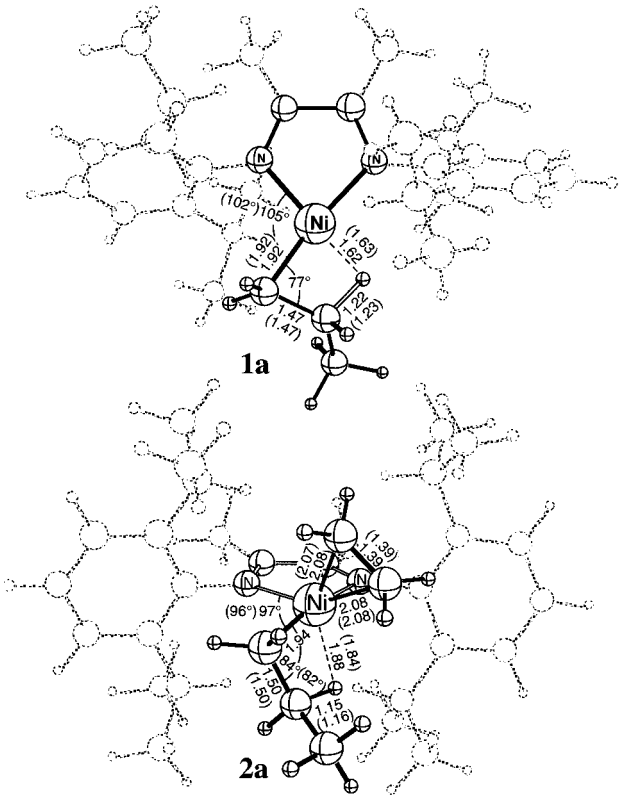

Figure 2. Optimized QM/MM metal alkyl cation and metal alkyl π-ethylene resting state structures. MM atoms (set 3 and set 4 atoms as defined in ref 12) are ghosted for clarity, while the dummy hydrogen atoms (set 2) are omitted. Parenthetic values refer to the same geometric parameter found in the corresponding pure QM geometry as described in ref 10. Distances and angles shown are in angstroms and degrees, respectively.

3. Results and Discussion

a. Propagation. i. Ni−Alkyl Complex and the Resting State. Displayed in Figure 2 are the optimized geometries of the most stable Ni−propyl cation, **1a**, and Ni−propyl π-ethylene, **2a**, conformations found. The pure MM atoms (set 3 and set 4 atoms) are ghosted for clarity, while the dummy hydrogen atoms (set 2) are omitted. Parenthetic values refer to the same geometric parameter found in the corresponding pure QM geometry as described in ref 10.

The QM domain (set 1 atoms) of the β-agostic Ni−alkyl complex, **1a**, remains essentially unchanged when compared to the pure QM model system. This is expected since the α-carbon and the β-agostic hydrogen atoms occupy the unencumbered square planar coordination sites of the Ni center as opposed to the sterically hindered axial sites (Figure 1). The most notable change upon introduction of the bulky diimine substituents is that the N−Ni−C_α angle is increased slightly from 102° in the pure QM model to 105° in the QM/MM model. We will see that this is a common effect of the bulky ligands as they tend to compress the groups within the active site together. The aryl rings are twisted away from a perpendicular orientation with respect to the Ni−diimine ring. This not only minimizes steric interactions with the alkyl chain, but there is also an electronic preference for this since the stabilizing interactions between π-systems of the Ni−diimine ring and the aryl rings are maximized when the rings are coplanar. In our model, this orientational preference of the rings is described by a molecular mechanics N−C(aryl) bond torsion potential. We note that a fully coplanar orientation of the rings cannot be achieved because of severe steric interactions incurred between

(31) Rappé, A. K.; Casewit, C. J.; Colwell, K. S.; Goddard, W. A., III; Skiff, W. M. *J. Am. Chem. Soc.* **1992**, *114*, 10024.
(32) Margl, P.; Ziegler, T. *Organometallics* **1996**, *15*, 5519.
(33) Margl, P. M.; Ziegler, T. *J. Am. Chem. Soc.* **1996**, *118*, 7337.
(34) Stanton, R. V.; Merz, K. M. J. *J. Chem. Phys.* **1993**, *100*, 434.
(35) Folga, E.; Ziegler, T. *J. Am. Chem. Soc.* **1993**, *115*, 5169.
(36) Li, J.; Schreckenbach, G.; Ziegler, T. *J. Phys. Chem.* **1994**, *98*, 4838.
(37) Ziegler, T.; Li, J.; Schreckenbach, G. *Inorg. Chem.* **1995**, *34*, 3245.
(38) Li, J.; Schreckenbach, G.; Ziegler, T. *J. Am. Chem. Soc.* **1995**, *117*, 486.
(39) Ziegler, T.; Li, J. *Can. J. Chem.* **1994**, *72*, 783.
(40) Matsubara, T.; Maseras, F.; Koga, N.; Morokuma, K. *J. Phys. Chem.* **1996**, *100*, 2573.

Chart 2

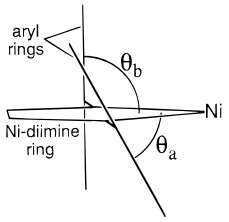

the aryl rings, the diimine ring, and both their substituents. Since the alkyl moiety of **1a** occupies the equatorial coordination plane, this allows the ortho-substituted aryl rings to twist away from the perpendicular alignment with the diimine plane. We quantify this twist with the angle, θ, between the aryl ring plane and the Ni−diimine ring plane as illustrated in Chart 2.[41] When θ is 90°, the rings are roughly perpendicular, and when θ is 0°, the rings are coplanar. In **1a** the θ angles are 64 and 68°.

Uptake of an ethylene unit by **1a** yields a Ni−alkyl π-olefin complex that has been shown by Johnson *et al.*[1] to be the resting state of the catalytic system. The most stable confirmation, **2a**, is sketched in Figure 2. Linear transit calculations[42] reveal that the resting state forms without a noticeable steric or electronic barrier when free ethylene is complexed to **1a**. This contrasts the conjecture of Brookhart and co-workers,[1,2] that the extreme bulk of the substituents hinders the complexation of the monomer. Here we suggest that the complexation barrier is entropic in nature, and that increases in the steric bulk of the substituents will act to increase the entropic barrier. This is supported by our linear transit calculations which show for the pure QM model system both axial and lateral attacks of the monomer are possible whereas for the QM/MM model only the lateral attack is possible. We are currently performing combined *ab initio* molecular dynamics and molecular mechanics calculations to address this issue.[43]

Although the parameters displayed in Figure 2 do not exhibit it to the full extent, the structure of the resting state, **2a**, is perturbed by the bulky ligands more so than the Ni−alkyl complex, **1a**. This is expected since the active site groups in the resting state occupy the axial positions, which are more sterically hindered than the equatorial sites. The steric demands of the aryl substituents act to bring the ethylene unit and the alkyl moiety closer together compared to the pure QM model. This is evidenced by a decrease in the $C_\alpha-C$(olefin) distances which are reduced to 2.88 and 2.90 Å in the QM/MM model from 2.92 and 2.95 Å in the pure QM model. The same is observed for the olefin midpoint−Ni−H_β angle, which is decreased to 108° from 116°. Expansion of the Ni−$C_\alpha-C_\beta$ angle and elongation of the Ni−H_β distance are also observed as a consequence of the compression of the active site units. This results in the weakening of the β-agostic bond as indicated in the shortening of the $C_\beta-H_\beta$ distance by 0.01 Å when the bulky ligands are introduced.

A related resting state structure, **2b** (not shown), that was located lies 1.4 kcal/mol above **2a**. The β-agostic resting states **2a** and **2b** differ by the orientation of the methyl group of the alkyl chain through a rotation about the $C_\alpha-C_\beta$ bond by approximately 60°. The rotational barrier linking **2a** and **2b** is expected to be very low since there is no steric hindrance to the process and since a stabilizing β-agostic interaction can be maintained throughout the rotation. For related polymerization catalysts, similar rotational barriers have been calculated and found to be less than 3 kcal/mol.[10,44,45] The bulky aryl ligands have a similar effect on **2b** as described for **2a**.

The bulky diimine substituents drastically reduce the calculated ethylene uptake energy. The ethylene complexation energy in **2a** is 14.7 kcal/mol whereas the most favorable uptake energy in the pure QM model was determined[10] to be 19.4 kcal/mol. Thus, the bulky ligands as modeled by the MM force field reduce the ethylene uptake energy by 4.9 kcal/mol. Over 95% of the change in uptake energy is accounted for by a destabilization exhibited in the MM contribution. In other words, changes in the QM electronic structure due to the perturbation of the geometry account for only 5% of the lowered uptake energy. A decomposition of the molecular mechanics energy which is summarized in Table 1 reveals that the destabilization can primarily be accounted for by two factors. First, as intuitively expected, there is an increased steric interaction between the active site fragments and the aryl rings. This occurs because both axial coordination sites of the metal are occupied in the resting state and therefore steric interactions involving the aryl rings and the active site fragments cannot be significantly reduced by rotation of the aryl rings. In particular, rotation of the rings, which may alleviate the steric hindrance between one of the ortho substituents and the top axial group, will only enhance the interaction between the other ortho substituent and the bottom axial group, and *vice versa*. To quantify the increase in steric interaction, we have analyzed the MM van der Waals interaction energy involving the aryl rings (including the *o*-isopropyl groups) and the propyl fragment of the active site. We find that there is a 1.20 kcal/mol increase in this interaction energy in going from **1a** to **2a**. The second dominant source of destabilization occurs because the aryl rings in the resting state are forced to adopt a less favorable perpendicular orientation with respect to the Ni−diimine ring. For example, the angles θ_a and θ_b between aryl ring planes and the Ni−diimine ring plane (see Chart 2) are 81° and 86° in the resting state, **2a**, whereas they are 64° and 68° in the Ni−alkyl cation, **1a**. As described earlier, the molecular mechanics N−C(aryl) bond torsion potential has a maximum at the perpendicular orientation and a minimum at a parallel orientation of the rings. This physically corresponds to the stabilizing interaction between the π-systems of the two rings, which is maximized at a parallel orientation. This rotation of the aryl rings with respect to the Ni−diimine ring destabilizes the MM torsion energy by 3.5 and 2.9 kcal/mol for the two rings, respectively.

The possibility that the resting state complex really possesses two coordinated monomer units (as opposed to one) which occupy each of the axial coordination sites of the metal center has been examined. We have found that the addition of a second olefin unit provides virtually no stabilization with $\Delta H = -0.5$ kcal/mol. Consequently, this auxiliary coordination is easily overcome by entropic factors, and we conclude that the single olefin π-complex is indeed the resting state.

ii. Insertion.[46] In both the pure QM and the hybrid QM/MM models, we find two distinct insertion channels which we

(41) The reported values are the angle between the normal vectors of the two planes defined by the Ni, N, C atoms of the Ni−diimine ring and C1, C2, C6 atoms of the aryl ring.

(42) Two linear transit calculations were performed in which one of the Ni−C(ethylene) distances was used as the reaction coordinate. The reverse process, from the resting state to the free Ni alkyl cation and free ethylene unit, was examined.

(43) Woo, T. K.; Margl, P. M.; Deng, L.; Blöchl, P. E.; Ziegler, T. Work in progress.

(44) Lohrenz, J. C. W.; Woo, T. K.; Ziegler, T. *J. Am. Chem. Soc.* **1995**, *117*, 12793.

(45) Woo, T. K.; Margl, P. M.; Lohrenz, J. C. W.; Ziegler, T. *J. Am. Chem. Soc.* **1996**, *118*, 13021.

(46) We have also examined the first insertion or chain initialization process with our pure QM/MM model. The first insertion of ethylene into the Ni−methyl bond is calculated to proceed through a barrier of 5.7 kcal/mol. This is significantly diminished from the pure QM model, which gives a first insertion barrier of 11.1 kcal/mol.

Table 1. Energy Decomposition for Insertion, Termination, and Isomerization Processes

species	ΔE_{TOT}[a]	ΔE_{MM}[a]	ΔE_{QM}[a]	ΔE[a,b] (pure QM)	ring plane angle, θ[c] a	ring plane angle, θ[c] b	$\Delta E_{torsion}$ (N−C1)[a,d] a	$\Delta E_{torsion}$ (N−C1)[a,d] b	ΔE_{vdw}[a,e] aryl substituents with ethene	propyl	methyl
insertion[f]											
2a	0.0	0.00	0.00	0.0	78	83	0.00	0.00	0.00	0.00	0.00
2b	1.4	0.44	0.96	−0.5	81	86	0.25	0.05	0.30	−0.29	0.11
1a + ethene	14.7	−4.87	19.57	−18.9	64	68	−3.54	−2.85		−1.20	−0.09
TS[2b-5]	13.2	−5.89	19.09	17.0	69	67	−2.48	−4.60	−0.21	0.02	0.35
TS[2a-5]	14.3	−5.32	19.62		70	68	−2.06	−4.37	−0.13	0.09	0.32
TS[3-6]	17.3	1.57	15.73	16.3	79	86	0.05	0.32	0.89	0.93	−0.07
termination[f]											
TS[2a-9]	18.6	4.80	13.80	9.2	89	89	0.90	0.36	1.56	1.25	1.54
TS[2b-9]	20.5	5.14	15.36	9.2	74	86	−0.64	0.31	1.14	0.25	1.56
isomerization[g]											
TS[1a-8]	15.3	4.01	11.29	12.8	64	88	0.42	3.19		1.12	−0.17
8	−0.8	0.06	−0.86	−1.8	69	71	0.53	0.43		−0.06	−0.23

[a] Energies are reported kcal/mol. [b] Relative energies of the analogous pure QM structures from ref 10. [c] The angle between the aryl rings and the Ni−diimine ring. Specifically, the angle θ is defined as the angle between the normal vectors of the two planes defined by atoms Ni, N, C(diimine) and C1, C2, C6, respectively. "a" and "b" refer to the each of the two aryl rings. [d] Relative molecular mechanics N−C1 bond torsion energies. "a" and "b" refer to each of the two aryl rings. [e] Relative molecular mechanics van der Waals interaction energy of the aryl fragments with the (i) ethene and (ii) propyl fragments of the active site and (iii) methyl fragment of the diimine ligand. [f] Energy components are relative to the resting state structure **2a**. [g] Energy components are relative to the Ni−propyl cation **1a**.

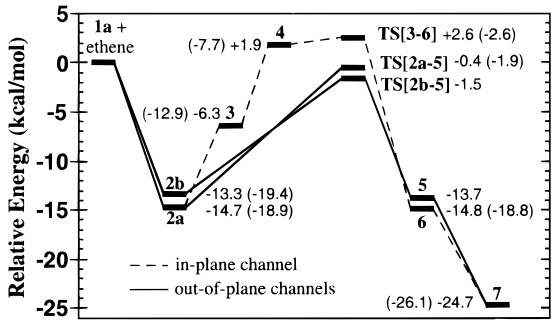

Figure 3. Energy profile for the chain propagation process. Parenthetic values refer to the analogous relative energies of the equivalent pure quantum mechanical structures of ref 10. All energies in kcal/mol.

have labeled the "in-plane" and "out-of-plane" insertion channels. Displayed in Figure 3 are the energy profiles of the out-of-plane insertion channels (solid) and the in-plane insertion channel (dotted). For the out-of-plane insertion we have explored two pathways, one initiated from the resting state structure **2a** and the other initiated from its rotamer **2b**.

The in-plane channel occurs in a stepwise fashion whereby two intermediate π-complexes are involved in addition to the incipient resting state π-complex, **2a**. The first intermediate observed, **3**, can be characterized as a π-complex in which the ethylene moiety is oriented perpendicular to the plane of the Ni−diimine ring. Rotation of the coordinated ethylene group in **3**, such that both carbon atoms lie in the diimine ring plane, yields the second intermediate **4**. Here, the alkyl group, the Ni−diimine fragment, and the ethene moiety are all coplanar. The optimized QM/MM structures of both these intermediates, **3** and **4**,[47] are shown in Figure 4. The bulky substituents act to destabilize the in-plane π-complexes, **3** and **4**, compared to their pure QM counterparts. Structures **3** and **4**, respectively, lie 8.4 and 16.6 kcal/mol higher in energy than the resting state structure **2a**, whereas the equivalent pure QM complexes lie 6.0 and 11.2 kcal/mol higher than the pure QM resting state. The most noticeable geometric consequence of the bulky ligands occurs in **4**, where the C_α−C(olefin) distance decreases from 2.65 Å in the pure QM complex to 2.44 Å in the QM/MM structure. Furthermore, the Ni−C_α−C_β angle increases from 133° to 140° as a result of the bulky aryl ligands. The transition state for the in-plane insertion, **TS[4-6]**, which is shown in

(47) The QM/MM structures **3** and **4** correspond to the pure QM structures **7a** and **8a** of ref 10.

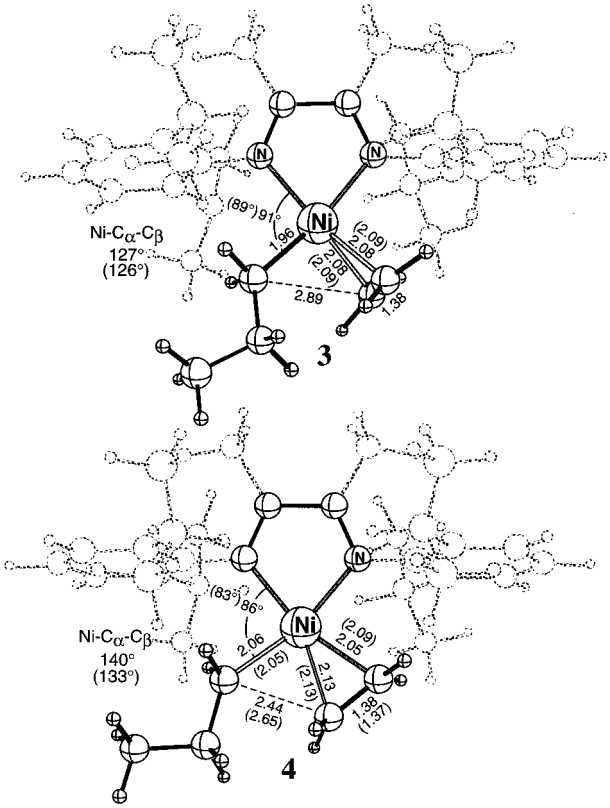

Figure 4. Optimized geometries of the intermediate π-complexes of the in-plane insertion channel. Conventions as in Figure 2.

Figure 5, lies 17.3 kcal/mol higher in energy than the resting state structure **2a**. This is only slightly higher than the 16.3-kcal/mol barrier observed with the pure QM system. Interestingly, the C(olefin)−C_α distance is actually 0.16 Å larger in **TS[4-6]** than in its pure QM counterpart. We suggest that an earlier transition state is formed due to the bulky groups. Since the in-plane insertion channel is less favorable than the out-of-plane channel when the bulky ligands are included, the transition states linking the π-complex **2a** to **3** and **3** to **4** were not located. We, however, do not expect these transformation barriers to be large based on our pure QM study[10] where these barriers were found to be less than 2 kcal/mol. The kinetic product of the in-plane insertion is a γ-agostic Ni−pentyl cation, **6**, which lies 1.0 kcal/mol above the resting state complex, **2a**. Species **6**,

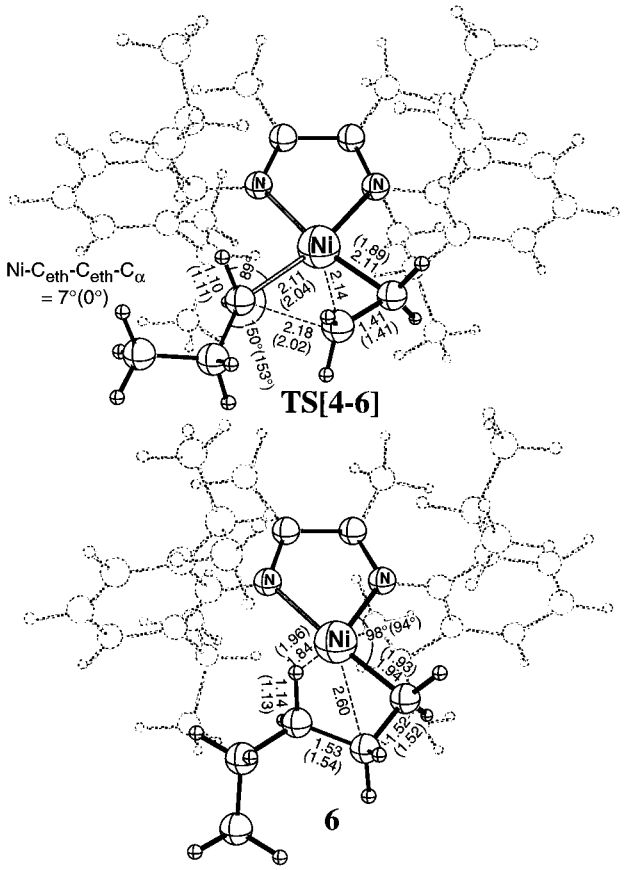

Figure 5. Transition state and kinetic product for the in-plane insertion channel. Conventions as in Figure 2.

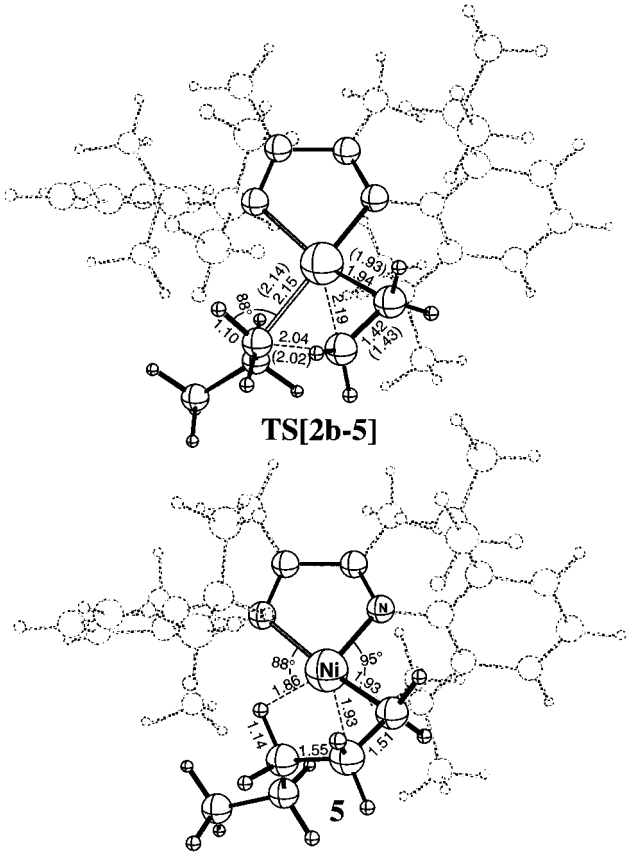

Figure 6. Transition state and kinetic product for the out-of-plane insertion channel. Conventions as in Figure 2.

which is pictured in Figure 5, has two γ-agostic hydrogens as evidenced by the short 1.84 and 1.99 Å Ni−H$_\gamma$ distances.

The insertion process in the second pathway, the "out-of-plane" channel, proceeds directly from the resting state structures and does not involve additional intermediary π-complexes. Here, the direct insertion initiated from both resting state conformations **2a** and **2b** has been explored. Although **2a** is the more stable of the resting states, the insertion transition state commencing directly from it lies slightly above the transition state derived from **2b**. As shown in Figure 3, **TS[2b-5]**, which lies 11.8 kcal/mol above the resting state **2b**, is 1.1 kcal/mol more stable than **TS[2a-5]**, which lies 14.3 kcal/mol above **2a**. Figure 6 displays the optimized QM/MM transition state structure **TS[2b-5]**. Since the interconversion of the two rotamers **2a** and **2b** is expected to be facile, it can be argued that the out-of-plane insertion commencing from the more stable resting state, **2a**, will likely lead to the more stable transition state, **TS[2b-5]**. Therefore, the most appropriate estimate of the out-of-plane insertion transition state is $\Delta H^{\ddagger} = 13.2$ kcal/mol. This value compares well with the experimental free energy barrier of propagation, which is estimated to be $\Delta G^{\ddagger} = 10-11$ kcal/mol.[48]

The analogous out-of-plane insertion process in the pure QM model system has a barrier of 17.5 kcal/mol.[10] Thus, the bulky substituents in the hybrid QM/MM model act to lower the out-of-plane insertion barrier by 4.3 kcal/mol. This is primarily due to the destabilization of the QM/MM resting state by the steric bulk of the aryl groups. More specifically, a more favorable orientation of the aryl rings with respect to the Ni−diimine ring in **TS[2b-5]** can be adopted compared to that in the resting state **2a**. As compiled in Table 1, these ultimately lead to a 5.9-kcal/mol decrease in molecular mechanics energy for **TS[2b-5]**. It is notable that for the pure QM model system, the in-plane insertion is calculated to be more favorable than the out-of-plane insertion—the opposite of what is presented here for the QM/MM system.

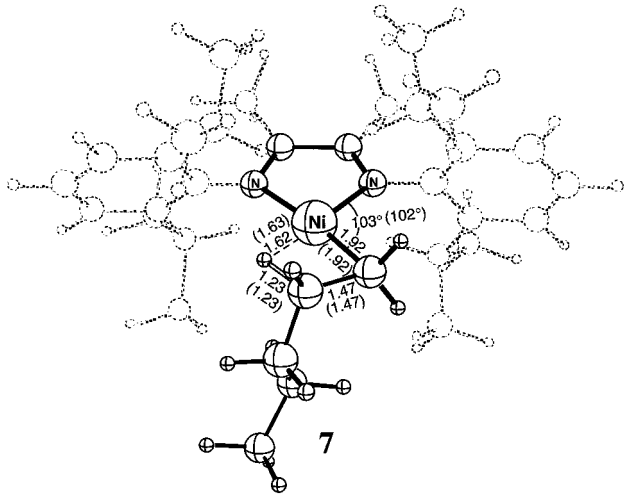

Figure 7. Optimized structure of the thermodynamic β-agostic insertion product. Conventions as in Figure 2.

The initial kinetic product of the out-of-plane insertion channel is a γ-agostic Ni−pentyl cation, **5**, which is displayed in Figure 6. Although **5** lies 1 kcal/mol above the resting state **2a**, it is likely to rearrange rapidly to form the thermodynamic β-agostic product **7**, which lies 11 kcal/mol below **5** and is sketched in Figure 7. We have not determined the transition state linking **5** to **7**. However, since the process is not sterically hindered by the bulky ligands, we expect the barrier to be very

(48) Professor Maurice Brookhart (Department of Chemistry, University of North Carolina at Chapel Hill). A private communication.

modest. For the pure QM model[10] and other related systems,[45] this rearrangement process from a γ-agostic metal−alkyl complex to a β-agostic complex is found to have a barrier of less than 3 kcal/mol. Structure **7** completes the propagation cycle, since we have calculated the monomer coordination and insertion process from β-agostic (**1a**) to β-agostic (**7**) Ni−alkyl complexes. The overall exothermicity of the insertion process (from **1a** + ethene to **7**) is $\Delta H = -24.7$ kcal/mol, which approaches the equivalent value of 26.1 kcal/mol in the pure QM model system.

From the hybrid QM/MM model, we conclude that the insertion barrier is 13.2 kcal/mol and proceeds directly from the resting state π-complex through the out-of-plane insertion channel. This is significantly diminished from the insertion barrier of the pure QM model system, which was determined to be 16.8 kcal/mol and proceeded through the stepwise in-plane channel. The primary effect of the bulky aryl ligands in the insertion process is to reduce the stability of the resting state complex, which results in a lowered insertion barrier. This is supported by the fact that relative to the reactant Ni−alkyl complex and free ethene molecule, the resting state is destabilized by 4.2 kcal/mol in the QM/MM model compared to the pure QM model, whereas both the insertion transition state and the thermodynamic product maintain their positions relative to the initial reactants in both the pure QM and QM/MM models. In other words, for both models the insertion transition states lie roughly 1−2 kcal/mol below the reactants and the thermodynamic products lie 25−26 kcal/mol below the reactants. This contrasts the resting state, which lies 14.7 kcal/mol below the reactants for the QM/MM model but 18.9 kcal/mol below the reactants for the pure QM system.

b. Chain Branching (Isomerization). Sketched in Scheme 2 is the proposed mechanism[1] that gives rise to the unique short-chain branching observed with the Brookhart catalyst systems. With this proposed mechanism, the branching occurs by a chain isomerization process whereby the β-hydrogen of the alkyl chain is eliminated, yielding a hydride olefin complex. Rotation of the π-coordinated olefin about the Ni−olefin bond followed by reattachment of the hydride produces a secondary carbon and, consequently, a branching point. Commencing from the monomerless Ni−alkyl cation, the pure QM calculations show that there is no stable hydride−olefin complex, thereby implicating a concerted isomerization pathway. A 12.8 kcal/mol isomerization barrier was determined for the pure QM model system. These calculations were repeated with the hybrid QM/MM model system, which was initiated from the β-agostic Ni−propyl cation, **1a**.

Concordant with the pure QM calculations, no stable hydride−olefin complex could be located. The optimized isomerization transition state, **TS[1a-8]**, lies 15.3 kcal/mol above **1a**. The bulky ligands, therefore, increased the isomerization barrier by 2.5 kcal/mol compared to the pure QM model system. Figure 8 shows that the isomerization transition state, **TS[1a-8]**, is somewhat compacted by the bulky aryl groups. This is illustrated by the slight compression of the $C_\beta-H_{hydride}$ and Ni−C_β distances and slight dilation of the N−Ni−C_α angle as a result of the introduction of the aryl ligands by the QM/MM method. The destabilization of the transition state due to the bulky ligands is not manifested in the electronic QM energy, but rather emerges in the MM energy. Again, there is a van der Waals component and a torsion component as detailed in Table 1. The torsional component arises because as the propene-like moiety rotates it forces one of the aryl rings to adopt an unfavorable perpendicular orientation such that the θ angle is 88° in **TS[1a-8]**.

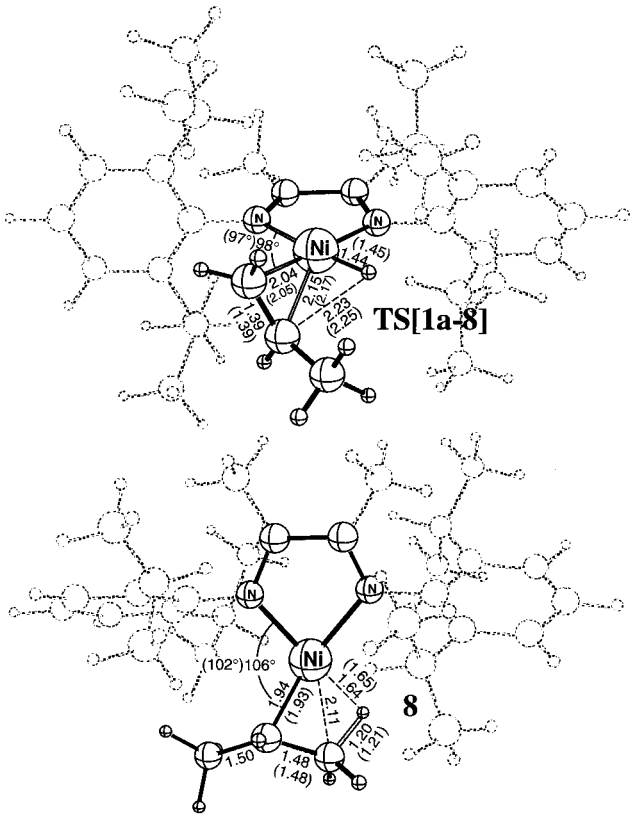

Figure 8. Transition state and product of the isomerization or chain branching process. Conventions as in Figure 2.

The overall QM/MM isomerization process is only exothermic by $\Delta H = -0.8$ kcal/mol, which is virtually unchanged from the pure QM system where the isomerization process is only 1 kcal/mol more exothermic with $\Delta H = -1.8$ kcal/mol. As summarized in Table 1, there is essentially no change in the MM energy between **1a** and the isomerization product, **8**. The 1 kcal/mol destabilization of the QM/MM isomerization product appears in the QM electronic energy. Figure 8, which depicts the optimized geometry of the isomerization product, reveals that the N−Ni−C_α angle is increased from 102° in the pure QM model to 106° in the hybrid model. Since there are no other significant changes in the geometry of the isomerization product, it is most likely this small perturbation in the active site that gives raise to the modest 1 kcal/mol decrease in the exothermicity of the isomerization process.

It is possible that chain isomerization could commence from the resting state, such that the isomerization occurs in the presence of the π-coordinated monomer. With our pure QM model system, we have located such a transition state that lies 3 kcal/mol higher than termination transition state. Since this transition state and the termination transition state are very similar in nature, the inclusion of the bulky aryl groups would make this process even more unfavorable. Therefore, our calculations show that the chain isomerization does not likely commence from the resting state.

c. Chain Termination. The chain termination is proposed to occur by an olefin assisted β-hydrogen elimination process. Brookhart and co-workers[1,2] have suggested that the termination is initiated by β-hydrogen transfer to the metal, to form an olefin hydride complex. In this picture, the termination is then completed by the association of monomer followed by insertion of the monomer into the metal−hydrogen bond. Since we could find no stable olefin hydride complex, we suggest that the termination is more concerted in nature such that the process is best described as a β-hydrogen transfer to the monomer. This

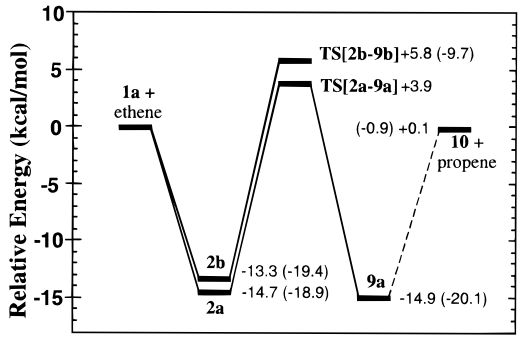

Figure 9. Energy profile for the chain termination process. Parenthetic values refer to the analogous relative energies of the equivalent pure quantum mechanical structures of ref 10. All energies in kcal/mol.

subtle variant is detailed in Scheme 3. Our earlier pure QM study of the termination reveals that the hydrogen transfer to the monomer involves a weak double π-olefin hydride complex whereby the transferred hydrogen is shared equally between the two olefin moieties which occupy the axial coordination sites. Neglecting the bulky ligands, the termination barrier was calculated to be 9.7 kcal/mol, significantly less than the pure QM propagation barrier of 16.8 kcal/mol. This is consistent with the fact that similar Ni and Pd systems which contain no bulky ligands are used as dimerization and oligomerization catalysts.[6−8]

In this study we have examined the termination process commencing from both resting states, **2a** and **2b**. The calculated QM/MM energy profiles are displayed in Figure 9. Unlike the termination process in the pure QM model, no discernible intermediate hydride complex could be located. Thus, in the QM/MM system the β-hydrogen is transferred directly from the alkyl chain to the monomer (compare Figure 9 with Figure 5 of ref 10). The termination pathway initiated from resting state structure **2a** leads to a 18.6-kcal/mol barrier, of which the optimized transition state, **TS[2a-9a]**, is displayed in Figure 10. The transition state, **TS[2b-9b]** (not shown), for the pathway initiated from **2b** lies 1.9 kcal/mol above **TS[2a-9]**, giving rise to a 19.1 kcal/mol barrier. These QM/MM termination barriers roughly double those of their pure QM counter parts. Table 1 reveals that there is a mutual destabilization exhibited in the QM electronic system and the MM system, which gives rise to the increased termination barrier in the QM/MM system. For example, the pure QM termination barrier is 9.7 kcal/mol, which compares to the change in the QM contribution of the total QM/MM energy of 13.8 kcal/mol for **TS[2a-9a]**. Thus, compared to the pure QM transition state, the electronic system of the QM/MM model is additionally destabilized by 4.1 kcal/mol. This perturbation of the electronic system by the bulky MM substituents is also evident in the geometric distortion of the transition state structure. Most notably, there is a contraction of the $C_\beta-H_{hydride}$ bond of 0.12 Å. The destabilization of the transition state due to the MM potential accounts for 4.8 kcal/mol, roughly half of the overall destabilization. The last three columns of Table 1 show that most of the MM destabilization is a result of an increased steric interaction between the aryl rings and the active site fragments (ethene and propyl). In addition to these steric interactions, there is an ~1.5-kcal/mol increase in the steric interaction between the aryl rings and the auxiliary methyl fragments bound to the diimine ligand. Thus, the substituents on the diimine ligand play an important role in destabilizing the termination transition state. It has been observed experimentally that if the diimine methyl groups are replaced by hydrogen atoms, the molecular weights decrease dramatically from 8.1×10^5 to 2.8×10^5 g·mol^{-1}.[1]

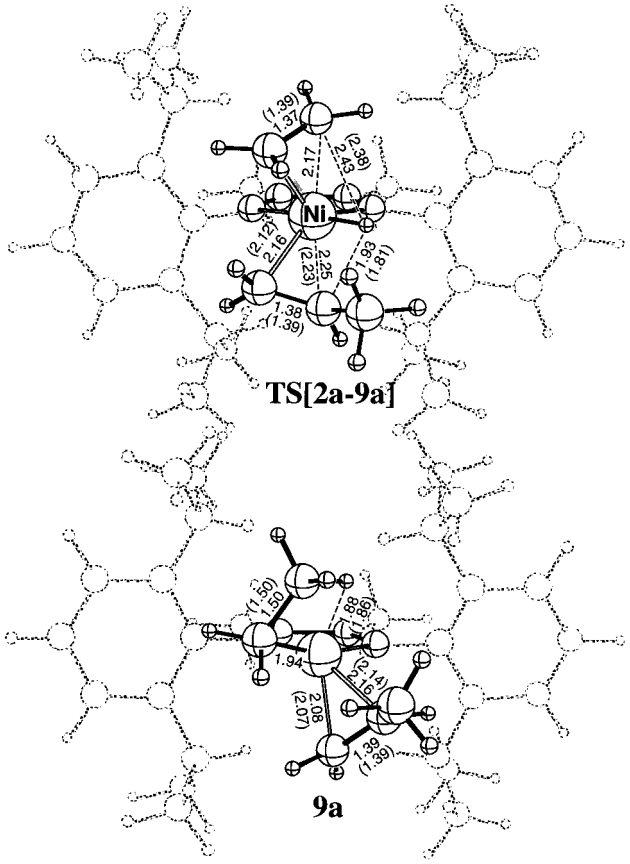

Figure 10. Transition state and product of the chain termination process. Conventions as in Figure 2.

d. Comparison of Theoretical and Experimental Results. The reaction barriers calculated from our combined QM/MM model are in excellent agreement with the experimentally determined free energy barriers, both in absolute and relative terms. This contrasts the results of the pure QM study where the bulky ligands were not modeled and the order of the barriers was not reproduced. The role of the bulky ligands can be examined in detail since we have two model systems, one in which the bulky aryl rings are modeled by a molecular mechanics potential and one where there are no bulky aryl rings.

i. Propagation. The calculated QM/MM propagation barrier of $\Delta H^\ddagger = 13.2$ kcal/mol agrees well with the experimental free energy barrier[48] of $\Delta G^\ddagger = 10-11$ kcal/mol. This compares with the calculated pure QM propagation barrier of 16.8 kcal/mol. As previously discussed, the bulky ligands act primarily to reduce the stability of the resting state while the energies of the thermodynamic product and the transition state remain unchanged relative to the Ni−alkyl cation. Thus, the polymerization activities should actually increase with increasing steric bulk. This peculiar effect has been observed experimentally.[1] For example, when the *o*-isopropyl groups are replaced by less bulky *o*-methyl groups, the catalyst activities are found to decrease from 7680 to 1800 kg per mol of Ni per h.

ii. Chain Branching (Isomerization). Table 2 summarizes the reaction barriers for the pure QM model system, the present QM/MM model system, and experimental results in both relative and absolute terms. Based on the frequency of secondary carbon atoms in the polymer chain as determined from NMR experiments, and assuming that the fraction of branching can be equated with the rate of isomerization, the isomerization barrier is estimated to be 1.3 kcal/mol greater than the insertion barrier. This is in reasonable agreement with our calculated QM/MM isomerization barrier of 15.3 kcal/mol, which lies 2.1 kcal/mol

Table 2. Comparison of Calculated Barriers to Experimental Relative Barriers

	reaction barriers (kcal/mol)		
	insertion	branching	termination
absolute			
pure QM[a] ($\Delta H^{\ddagger}$)	16.8	12.8	9.7
QM/MM ($\Delta H^{\ddagger}$)	13.2	15.3	18.6
exptl[b] ($\Delta G^{\ddagger}$)	10−11		
relative to insertion			
pure QM[a] ($\Delta\Delta H^{\ddagger}$)	0.0	−4.0	−7.1
QM/MM ($\Delta\Delta H^{\ddagger}$)	0.0	2.1	5.4
exptl[c] ($\Delta\Delta G^{\ddagger}$)	0.0	1.3[d]	5.6[e]

[a] Reference 10. [b] Reference 48. [c] Reference 1. Polymerization of 1.6×10^{-6} mol of (ArN═C(R)C(R)═NAr)Ni(CH_3)(OEt_2)]$^+$[B(3,5-$C_6H_3(CF_3)_2)_4$]$^-$ where Ar = 2,6-C_6H_3(*i*-Pr)$_2$ and R = Me in 100 mL of toluene at 0 °C for 15 min. [d] NMR studies provide a ratio of 48 isomerization events per 500 insertions, assuming that all branches are methyl branches (methyl branches are experimentally observed to predominate). Applying Boltzmann statistics to this ratio at 273.15 K yields a $\Delta\Delta G^{\ddagger}$ of 1.3 kcal/mol. [e] The weight-average molecular weight, M_w, of 8.1×10^5 g/mol provides an estimate for the ratio of termination events to insertion events of 1:28900. Using Boltzmann statistics to this ratio gives a $\Delta\Delta G^{\ddagger}$ of 5.6 kcal/mol.

above the calculated insertion barrier. We note that monomer concentration effects are not taken into account in our model and therefore the above comparison is dubious since the extent of branching may be highly dependent on the rate of monomer trapping. It has been demonstrated experimentally[1] that increasing the steric bulk of the ortho substituents increases the branching frequency. This is somewhat at odds with our theoretical result, which shows that there is a modest increase in the isomerization barrier of 2.5 kcal/mol in moving from the bare QM system which has no steric bulk to the hybrid QM/MM model. We therefore conclude that the dominant role of the bulky groups (pertaining to the branching process) is to impede the formation of the resting state, thereby promoting the branching process to occur.[49] To address the issue we are currently examining the process with the combined QM/MM *ab initio* molecular dynamics method.[43]

iii. Chain Termination. Our model systems show that of all the processes studied, the bulky ligands have the most dramatic effect on the termination, virtually doubling the termination barriers in going from the pure QM system to the QM/MM system (Table 2). This is in agreement with the fact that without the bulky ligands these Ni diimine systems are mere dimerization catalysts, but with the bulky ligands these systems are commercially viable polymerization catalysts. Our theoretical results are also in agreement with the related finding that as the steric bulk of the diimine ligands is increased, there is a correspondent increase in the molecular weights. As previously discussed, our analysis of the destabilizing interactions in the termination transition state reveals that the methyl groups bound to the diimine ligands interact strongly with the bulky aryl substituents. Again this is consistent with the experiments which show that the polymer molecular weights drop when the methyl groups are replaced by hydrogens.

From the weight-average molecular weight, M_w, we can estimate the ratio of termination events to insertion events, which can in turn be used to determine the difference between the termination and insertion free energy barriers, $\Delta\Delta G^{\ddagger}$. As shown in Table 2, there is a remarkable agreement between the experimental ($\Delta\Delta G^{\ddagger}$ = 5.6 kcal/mol) and QM/MM ($\Delta\Delta H^{\ddagger}$ = 5.4 kcal/mol) termination barrier relative to the insertion.

(49) This is further corroborated by the experimental observation that increased ethylene pressures decrease the branching, while not dramatically affecting the polymer yields or molecular weights.

In calculating $\Delta\Delta G^{\ddagger}$ we have assumed that every hydrogen transfer event leads to the loss of the chain and, consequently, chain termination. However, the vinyl terminated chain in **9a** can reinsert. If the reinsertion is competitive with chain loss then the above assumption is invalid. Other polymerization systems, namely early transition metal metallocenes, generally exhibit the behavior that the higher the α-olefin, the higher the barrier to insertion.[50] This would pin point the reinsertion barrier to be at least as high as the normal monomer insertion barrier. In the worst case, this would imply that our assumption is incorrect. Here, we argue that our chain loss barrier is a gas phase barrier and that the loss of olefin is in actuality assisted by the solvent or ethylene, resulting in a barrier substantially lower than that in the gas phase. This further implies that the barrier to olefin loss is significantly lower than the barrier to reinsertion and, consequently, indicates that our approximation is justifiable.

e. General Discussion. For the Brookhart catalyst system the combined QM/MM method is clearly an improvement over the truncated pure QM model because of the critical importance of the bulky aryl substituents which are neglected in the pure QM model. Our calculations further show that the QM/MM model is a clear improvement over a stepwise QM followed by MM method.[51−55] In the stepwise QM/MM method, QM calculations are first performed by using a truncated model system in which the bulky substituents are neglected. Then a MM calculation is performed on the whole system with use of active site geometries extracted from the pure QM calculation. The most important difference between the stepwise QM/MM method and the present combined QM/MM method is that during geometry optimization in the stepwise method, the pure QM geometry is fixed.[56] Therefore, there is no relaxation of the active site structure in order to accommodate the bulky substituents. For the sake of comparison, we have performed such a stepwise QM/MM calculation whereby the pure QM geometry of ref 10 was frozen in an MM calculation by using the same force field as described above. The results of the stepwise QM/MM calculations are poor. For example, the barriers for insertion, branching, and termination are $\Delta H^{\ddagger}$ = 18.5, 14.0, and 25.7 kcal/mol, respectively. This compares to $\Delta H^{\ddagger}$ = 13.2, 15.8, and 18.6 kcal/mol, respectively, for the combined QM/MM method. Another noteworthy result of the stepwise QM/MM method is that it overestimates the energy difference between the two resting state rotamers **2a** and **2b**. The stepwise method predicts that **2a** is 5.3 kcal/mol more stable than **2b** whereas the combined QM/MM results provide a difference of 1.0 kcal/mol. We conclude that for this system full optimization of both the QM and MM regions, as is done in the combined QM/MM method, is necessary to provide even qualitatively correct results.

The primary goal of this study was to examine, in detail, the role that the bulky substituents play in the polymerization chemistry of the Brookhart Ni−diimine catalysts. By simple examination of the catalyst structure one can ascertain that the bulky substituents block the axial coordination sites. Our previous pure QM study, which revealed the nature of the

(50) Brintzinger, H. H.; Fischer, D.; Mülhaupt, R.; Rieger, B.; Waymouth, R. M. *Angew. Chem., Int. Ed. Engl.* **1995**, *34*, 1143.
(51) Cavallo, L.; Guerra, G. *Macromolecules* **1996**, *29*, 2729.
(52) Hart, J. R.; Rappé, A. K. *J. Am. Chem. Soc.* **1993**, *115*, 6159.
(53) Castonguay, L. A.; Rappé, A. K. *J. Am. Chem. Soc.* **1992**, *114*, 5832.
(54) Morokuma, K.; Yoshida, T.; Koga, N. *Organometallics* **1996**, *15*, 2766.
(55) Kawamura-Kuribayashi, H.; Koga, N.; Morokuma, K. *J. Am. Chem. Soc.* **1992**, *114*, 8687.
(56) Comparison of the combined QM/MM and the stepwise QM then MM methodologies can be found in ref 40.

generic intermediates and transition states involved, suggested that the bulky ligands would have the most dramatic effect on the termination process that utilizes both axial coordination positions. This combined QM/MM study reaffirms this picture. Analysis of the molecular mechanics energy contributions as previously discussed suggests that there is a second important feature of the aryl ligands apart from the positioning of the steric bulk. We observe that preferential orientation of the aryl rings away from a perpendicular alignment to the Ni−diimine ring provides stabilization in both the Ni−alkyl complexes and the insertion transition states. This factor contributes to the reduction of the propagation barrier as compared to the pure QM model system. It is difficult to ascertain the relative importance of this secondary effect since strong steric effects can often manifest themselves in other molecular mechanics energy terms, such as bond bending and torsion energy terms. Despite this, we suggest that increasing the preference for a more parallel alignment of the aryl rings by increasing the π-orbital interactions between the aryl rings and the diimine ring will have an effect of increasing the activity of the catalyst and increasing the molecular weights. This can be achieved (other ramifications not considered) by substitution of the para hydrogen of the aryl ring by an acceptor group such as $-NO_2$ or $-CF_3$. Another possibility is to functionalize the diimine R group such that it interacts with the *o*-isopropyl group so as to pull the aryl rings into a more coplanar orientation. Unfortunately, our model suggests that this would also lead to diminished branching since the isomerization TS has a destabilizing torsional component.

In the current QM/MM model, the electrostatic coupling between the QM and MM atoms has been neglected. In some systems this approximation may be severe. However, in the present case we feel that this approximation is justified since the dominant nonbonded interactions between the QM (ethene and propyl moieties) and MM (isopropyl and methyl groups) regions do no involve any highly polarized groups. The good agreement between the calculated and experimental results further suggests that this approximation is reasonable in this case.

4. Conclusions

We have successfully applied the combined QM/MM methodology of Morokuma and Maseras[12] to the study of the Brookhart Ni(II) diimine ethylene polymerization catalysts of the type (ArN═C(R)−C(R)═NAr)$Ni^{II}-R'^{+}$, where R = Me and Ar = 2,6-C_6H_3(*i*-Pr)$_2$. In the combined QM/MM model, the bulky Ar and R groups were treated by a molecular mechanics potential while the remainder of the system was treated by density functional theory (Becke88-Perdew86). Chain propagation, chain branching, and chain termination were studied and calculated to have barriers of $\Delta H^{\ddagger} = 13.2$, 15.3, and 18.6 kcal/mol, respectively. These calculated barriers are in remarkable agreement with experiment in both absolute and relative terms. This contrasts our earlier pure QM study, which neglects the bulky ligands. Here, the propagation, branching, and termination barriers were calculated to be $\Delta H^{\ddagger} = 16.8$, 12.8, and 9.7 kcal/mol, respectively, which is the reverse order of barriers as that determined experimentally. In the present QM/MM study, we find that the bulky ligands act to destabilize the resting state complex. This has the effect of *lowering* the insertion barrier since the relative energy of the insertion transition state is not significantly perturbed by the bulky substituents. With respect to the chain branching and chain termination processes, the bulky ligands destabilized the transition states. This is particularly true of the termination process in which there is a 2-fold increase in the barrier.

With our pure QM and the present QM/MM study we are able to reproduce the experimental observation that the generic Ni(II) diimine systems are intrinsically dimerization catalysts, but can be converted into polymerization catalysts with the addition of suitable substituents. Our study suggests that two criteria need to be met by the bulky substituents for this to be successful. First and foremost, the substituents must disproportionately block the axial coordination sites of the Ni center over the equatorial coordination sites, as was first suggested by Johnson *et al.*[1] Secondly, our calculations suggest that the substituents must also have a conformational preference to vacate the axial sites. In the particular case of the aryl ring substituents, it is more favorable for the rings to orient themselves (more) parallel to the Ni−diimine plane than to remain perpendicular to it.

Finally, we conclude that the combined QM/MM method can be effectively applied to a study of transition metal based catalytic processes in a detailed and efficient manner. Moreover, we have demonstrated that the unique features of the QM/MM method have allowed for deeper insights into the substituent effects to be achieved compared to either the truncated pure QM model or the stepwise QM then MM model.

Acknowledgment. This work has been supported by the National Sciences and Engineering Research Council of Canada (NSERC), as well as by the donors of the Petroleum Research Fund, administered by the American Chemical Society (ACS-PRF No. 31205-AC3) and by Novacor Research and Technology Corporation (NRTC) of Calgary. The authors acknowledge valuable comments of NRTC scientists Drs. L. Fan, D. Harrison, R. Spence, and J. McMeeking. L.C. thanks The University Federico II of Naples for financial support within the "Programma di Scambi Internazionali". P.M.M. would like to thank the Austrian Fonds zur Förderung der wissenschaftlichen Forschung (FWF) for financial support within project JO1099-CHE. T.K.W. wishes to thank NSERC, the Alberta Heritage Scholarship Fund, and the Izaak Walton Killam Memorial Foundation for graduate fellowships.

Supporting Information Available: Cartesian coordinates of all species mentioned in the text and a full listing of the molecular mechanics force field parameters utilized (9 pages). See any current masthead page for ordering and Internet access instructions.

JA970226A